Smart Structures and Systems, *Vol. 25, No. 3 (2020) 323-335*
DOI: https://doi.org/10.12989/sss.2020.25.3.323

Feasibility of a new hybrid base isolation system consisting of MR elastomer and roller bearing

Yongmoon Hwang [1a], Chan Woo Lee [2b], Junghoon Lee [1c] and Hyung-Jo Jung*[1]

[1] *Department of Civil and Environmental Engineering, Korea Advanced Institute of Science and Technology, 291 Daehak-ro, Yuseong-gu, Daejeon 34141, Republic of Korea*
[2] *Department of Civil and Environmental Engineering, Korea Army Academy at Yeong-cheon, Yeong-cheon 38900, Republic of Korea*

(*Received October 3, 2019, Revised December 31, 2019, Accepted January 9, 2020*)

Abstract. Magnetorheological elastomer (MRE), a smart material, is an innovative material for base isolation system. It has magnetorheological (MR) effect that can control the stiffness in real-time. In this paper, a new hybrid base isolation system combining two electromagnetic closed circuits and the roller bearing is proposed. In the proposed system, the roller part can support the vertical load. Thus, the MRE part is free from the vertical load and can exhibit the maximum MR effect. The MRE magnetic loop is constructed in the free space of the roller bearing and forms a strong magnetic field. To demonstrate the performance of the proposed hybrid base isolation system, dynamic characteristic tests and performance evaluation were carried out. Dynamic characteristic tests were performed under the extensive range of strain of the MRE and the change of the applied current. Performance evaluation was carried out using the hybrid simulation under five earthquakes (i.e., El Centro, Kobe, Hachinohe, Northridge, and Loma Prieta). Especially, semi-active fuzzy control algorithm was applied and compared with passive type. From the performance evaluation, the comparison shows that the new hybrid base isolation system using fuzzy control algorithm is superior to passive type in reducing the acceleration and displacement responses of a target structure.

Keywords: Magnetorheological Elastomer (MRE); Magnetorheological (MR) effect; hybrid base isolation system; semi-active control; hybrid simulation

1. Introduction

Protecting the infrastructures from hazard ground vibration is an important factor in maintaining lives and sources. The concept of base isolation was introduced to protect structures from natural disasters such as earthquakes. It is to isolate the structure from unexpected vibration of the ground by inserting a structural member with horizontal stiffness between the structure and the foundation (Naeim and Kelly 1999, Skinner *et al.* 1993). A general seismic resistance that can attaches thick and strong stiffeners is the way to survive an earthquake, while the base isolation is a way to avoid earthquakes by isolating the structure from the ground. The general seismic resistance causes high responses of the acceleration and displacement in the top floor when earthquake occurs. However, the external force is not transmitted to the top floor and the entire building moves slowly in the base isolation system (Tiong *et al*. 2017). The conventional base isolation systemis a passive type in which characteristics are determined in anticipation of earthquakes. In other words, an unexpected earthquake can occur severe problems in structures. Also, several researches have revealed that the conventional base isolation system can be vulnerable for near-fault earthquake (Jangid and Kelly 2001, Nagarajaiah 2006 and Domizio *et al*. 2019). To address these problems, adaptive hybrid base isolation systems have been proposed. Yoshioka *et al*. (2002) and Ramallo *et al*. (2002) have proposed a system that combines MR fluid attenuator with a conventional base isolation device. Wongprasert and Symans (2005) have experimented and evaluated the multi-layer structure frame by combining laminated rubber bearings with variable-orifice fluid dampers. However, the additional installation of the damper complicates the construction and the excessive displacement of the damper increases the responses of the inter-layer displacement and acceleration (Naeim and Kelly 1999). In the meantime, one of the smart materials called magnetorheological elastomer (MRE) not only overcomes the shortcomings of the existing base isolation system, but also introduces a new type of base isolation system to control the stiffness and damping ratio. The change of damping ratio of the MRE under the magnetic field is negligible compared with the change of stiffness (Ginder *et al*. 2000). The MRE has a magnetorheological (MR) effect that modulates the elastic modulus through the application of a magnetic field (Jolly *et al*. 1996, Davis 1999, Lokander and Stenberg 2003, Ruddy *et al*. 2012, Zhang and Li 2009). Their response time is less than ten milliseconds (Ginder *et al*. 2000). This has the potential of a smart base isolation system that can adapt in real time to a variety of external excitation. Thus, the MR

*Corresponding author, Professor,
E-mail: hjung@kaist.ac.kr
[a] Ph.D. Student, E-mail: yongmoon@kaist.ac.kr
[b] Lecturer, E-mail: 3academy4923@army.mil.kr
[c] Ph.D., E-mail: jhlee07@kaist.ac.kr

Copyright © 2020 Techno-Press, Ltd.
http://www.techno-press.org/?journal=sss&subpage=7
ISSN: 1738-1584 (Print), 1738-1991 (Online)

effect can be calculated using the change of the elastic modulus depending on the magnetic field. The MR effect has been discovered by Jacob Rabinow (Clutch and Rabinow 1948, Rabinow 1951). It can be expressed as

$$MR\ effect\ (\%) = \frac{G(B_{MRE}) - G(0)}{G(0)} \times 100 \quad (1)$$

where $G(B_{MRE})$ and $G(0)$ are the shear elastic modulus with / without a magnetic field. The control of the elastic modulus enables the adjustment of the natural period of the base isolated structure.

The major factors that greatly influence the MR effect are the volume fraction, shape and size of the magnetic particles. Lokander and Stenberg (2003) have compared the MR effects of different magnetic particle types. In addition, the MR effect comparison has been performed according to the volume fraction of the magnetic particles. In this study, the MRE specimen is fabricate based on Lee (2018) and Lee *et al*. (2018). Lee (2018) and Lee *et al*. (2018) have performed the fabrication and characterization of the MRE depending on the volume fraction of the magnetic particle which shows the highest MR effect among the several magnetic particles (Lokander and Stenberg 2003).

The MRE has the property of being an innovative alternative to the material of the base isolation system, and several researches have proposed the base isolation system based on the MRE. However, there are no practical cases yet, and it is necessary to supplement it for realistic purposes. The elements to be required for the base isolation system are as follows: (i) support vertical load, (ii) deformation of the MRE at wide range of strain, and (iii) optimal mixture ratio. As a base isolation system, it is important to have a robust vertical stiffness to support structures (i). According to ISO 22762-1, the shear modulus of the base isolation is to be measured at 100% strain amplitude (ii). Also, the MRE should be fabricated by the proper material with optimal mixture ratio to obtain the maximum MR effect (iii). The detailed information related to (i) ~ (iii) is described in the next section.

Behrooz *et al.* (2014a, b) have proposed a variable stiffness and damping isolator (VSDI) as shown in Fig. 1(a). Four trapezoidal MREs are formed and coils are placed up and down of the MRE. The steel shims, rubber, and MRE are placed in the middle of the device to maintain the similarity of traditional steel rubber bearings and provide the fail-safe feature. The role of steel shim is to build a channel for magnetic flux passing through MREs with a higher magnetic field and to prevent tearing of the elastomeric layer to large deformation. The size of the device is 128 mm × 64 mm × 110 mm. the number of each coil is 800 turns. The performance of the proposed device was evaluated using a scaled down three-story building under El Centro earthquake. However, in that study, (i) and (iii) of the above mentioned factors arise in the problems of base isolation system based on the MRE (Chen *et al*. 2007, Li *et al*. 2014).

Also, the laminated MRE-based base isolation device has been proposed (Li *et al*. 2013, Li and Li 2019). In this design, 46 layers of 1 mm thick steel plates and 47 layers of 2 mm thick MRE sheets are used with the same diameter 140 mm (Li *et al*. 2013). The coil is placed outside the laminated bearing element. The solenoid consists of an electromagnetic coil and a thin non-magnetic support as shown in Fig. 1(b). The overall size of the device is Φ 232 mm × 276 mm with the laminated structure of thin steel and MRE layers (Φ 140 mm × 137 mm). Characteristic tests were performed according to the change of frequency, applied current, and displacement. Also, the performance of the device under 380 kg load test was carried out with the limited strain up to 27.7% (i.e., deformation of the MRE only). However, there are limitations related to (ii) and (iii) (Chen *et al*. 2007).

To address above mentioned factors, a new hybrid base isolation system is proposed in this study. To support vertical load, the roller bearing system that is composed of roller/slider part in two axes is used and combined with the MRE electromagnetic closed circuits. Dynamic characteristic tests were carried out according to the change of strain (up to 100%) and the applied current (0.0, 2.5, 5.0 A). Detailed description of the proposed hybrid base isolation system is explained in the next section.

In addition, the performance evaluation of the proposed hybrid base isolation system was carried out under several earthquakes using passive and semi-active fuzzy control algorithm. Semi-active control can compensate for limited control range caused by passive control and address excessive power consumption in active control. There are few algorithms can be used effectively because of the nonlinearity of the MRE. On-off algorithm is one of the algorithms that are widely used (Liao *et al*. 2001, Zhu and Rui 2014). Clipped-optimal control strategy was used as

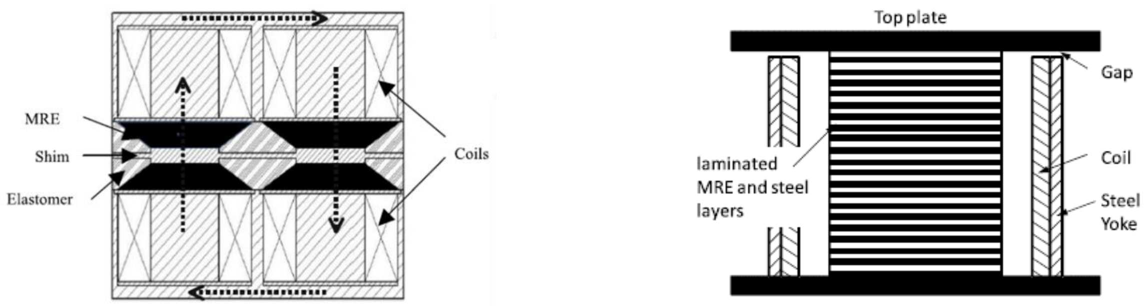

(a) (b)

Fig. 1 Base isolation system based on the MRE; (a) Behrooz *et al.* (2014a, b); and (b) Li *et al*. (2013)

semi-active control algorithm in Opie and Yim (2011). Behrooz *et al*. (2014b) have carried out the performance evaluation of the base isolation using the Lyapunov-based control strategy. Jung *et al*. (2011) have implemented fuzzy algorithm in a scaled structure. In this study, a two-story shear building isolated with the proposed hybrid base isolation system is investigated using hybrid simulation. Semi-active fuzzy control algorithm is suggested for this work and based on the relative displacement difference between base and 2nd floor, base floor displacement and velocity of earthquake. The results from fuzzy control algorithm are compared with those of passive type.

2. Hybrid base isolation system consisting of the MRE and roller bearing

2.1 Considerations for base isolation system based on the MRE

The base isolation system based on the MRE is a specified application of vibration isolation for civil engineering to prevent earthquakes from transmitting damage energy to protect structure. As the base isolator, it is required to have flexible lateral stiffness. The reason why the flexible lateral stiffness needs is to allow flexibility during earthquakes thus protecting the building by preventing dangerous motions. Fig. 2 shows the conventional MRE-based base isolation system. It is composed of the laminated MRE with steel plate like conventional rubber bearing, and combining the electromagnet coils surrounding the MRE. As mentioned in the previous section, the elements to be equipped for the base isolation system are as follows; (i) support vertical load, (ii) deformation of the MRE at wide range of strain, and (iii) optimal mixture ratio.

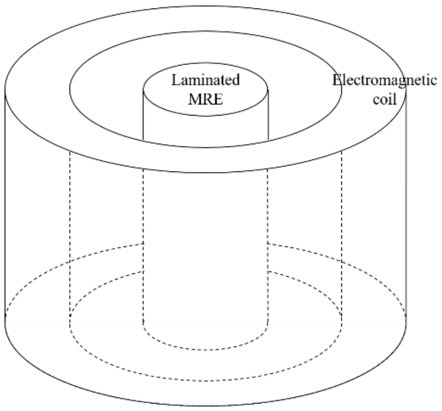

Fig. 2 Conventional base isolation system based on the MRE

(i) ‘Support vertical load’: it is a system that requires the infrastructure to be placed on the base isolation based on the MRE, which is flexible for horizontal stiffness but robust for vertical stiffness. Therefore, base isolation system based on the MRE should support the vertical load and be flexible for the horizontal load.

(ii) ‘Deformation of the MRE at wide range of strain’: deformation of the MRE against earthquake should be constructed to operate under a wide range of strain to prevent the MRE from tearing. According to ISO 22762-1, the shear modulus of the base isolation system is specified as 100% strain. Therefore, when performing the dynamic characteristic tests of the base isolation system, the dynamic characteristic tests should be carried out up to 100% strain.

(iii) ‘Optimal mixture ratio’: since the MRE exhibits the different MR effect depending on the material properties, it is necessary to carry out the study considering the optimal mixture ratio. The factors that mainly affect the MR effect are the volume fraction, size, and shape of the magnetic particles. Considering the factors affecting the MR effect, it is necessary to fabricate the MRE specimen with the proper ingredients and optimal mixture ratio.

2.2 Design and character of the proposed hybrid base isolation system

Figs. 3 and 4 show a schematic of the proposed hybrid base isolation system. The size of the proposed hybrid base isolation system is 400 mm × 360 mm × 220 mm. It consists of two electromagnetic closed circuits with the four MREs (Φ 40 mm × 20 mm), and the roller bearing (i.e., roller/slider part). Two controllers are connected to each electromagnetic closed circuit to apply a current up to 5 A (Fig. 3(b)). Each electromagnetic closed circuit divides MREs into two parts and connects them in series to minimize the size. Also, each electromagnetic coil has 1,830 turns with Φ 2.0 mm. It is realistic by installing

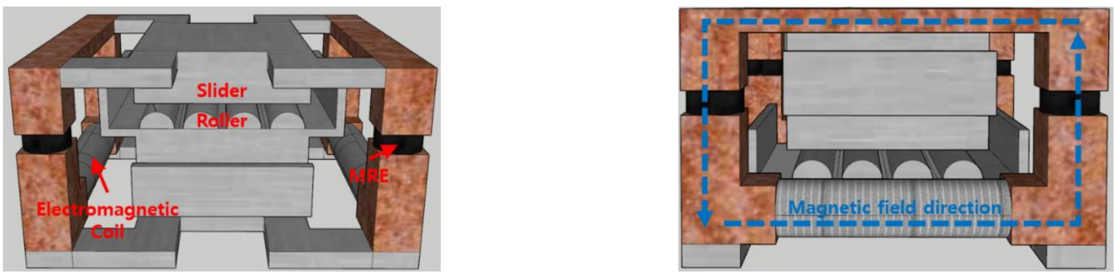

(a) (b)

Fig. 3 Components of the prototype; (a) Roller/slider part; and (b) MRE magnetic closed circuit

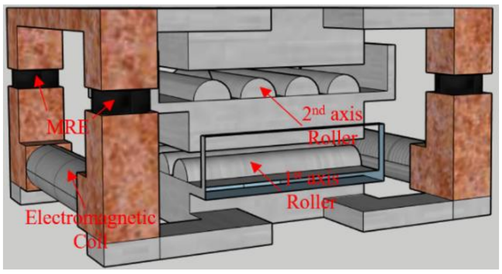

Fig. 4 Prototype of the proposed hybrid base isolation system consisting of the MRE and roller bearing

Table 1 Volume and Mass ratio of the MRE (Lee *et al*. 2018)

	Rubber (SVR CV60)	Iron (ASC 300)	Carbon black (N550)	Naphthenic Oil (N2)	Etc.
Volume ratio (%)	37.1	35.0	11.3	14.9	1.7
Mass ratio (%)	10.2	78.5	6.1	4.1	1.1

electromagnetic closed circuits in the free space generated by the roller/slider part. The fabrication of the MRE is based on Lee *et al*. (2018) and related information is tabulated in Table 1.

Several factors to be base isolation system based on the MRE and limitations of previous studies have described in the previous chpater. In this chpater, a new hybrid base isolation system that can take into account the factors mentioned above is described. The conceptual design of the proposed hybrid base isolation system is shown in Fig. 4. The proposed hybrid base isolation system is composed of two parts; (a) the MRE electromagnetic circuit and (b) the roller/slider part. The features of the proposed system are as follows:

(i) 'Support vertical load': by combining the roller/slider part with the MRE magnetic loop (Fig. 3), the vertical load is supported by the roller part (Son 2008 and Park *et al*. 2013), and the MRE can control in the horizontal direction (Fig. 3(a)). Also, the roller/slider part has almost zero horizontal stiffness to have flexibility in the horizontal direction, so that the MRE can effectively exhibit the MR effect. In addition, the roller bearing can behave up to the maximum deformation of the MRE. The fail-safety can be considered in that the roller bearing can be used as a passive-type base isolation system although the MRE is torn. Also, one of 40~60 mm roller can support a load of about 17.5 tons vertical load according to the specification of isolation roller bearing system (Son 2008). Since the roller bearing supports the vertical load, the MRE can be attached and detached when the MRE is degradation of torn. Fig. 5(a) shows an actual building isolation roller bearing system, and Fig. 5(b) shows the roller/slider part for the axial direction of the proposed hybrid base isolation system. In addition, two axes control is possible by constructing the roller/slider part in two axes as shown in Fig. 4.

(ii) 'Deformation of the MRE at wide range of strain': each electromagnetic circuit divides MREs into two parts and connects them in series to minimize the size as shown in Fig. 3. It is a realistic design because it is arranged by utilizing the free space created by the roller/slider part. The roller/slider part is designed to move within the limit motion range of the MRE, preventing the breakage of the MRE, and does not affect the movement of the MRE. In addition, characteristic tests of the proposed device were performed up to 100% strain according to ISO 22762-1.

(iii) 'Optimal mixture ratio': the MRE specimen is fabricated based on Lee *et al*. (2018). The MRE was fabricated using natural rubber (SVR CV 60) which has superior mechanical properties (Chen *et al*. 2007) and high usability and iron powder (ASC 300) which can exhibit the maximum MR effect among iron powders (Lokander and Stenberg 2003). As an additive, carbon black (N550) and naphthenic oil (N2) were used to enhance the MR effect. Detailed description related to fabrication of the MRE specimen is referred in Lee *et al*. (2018).

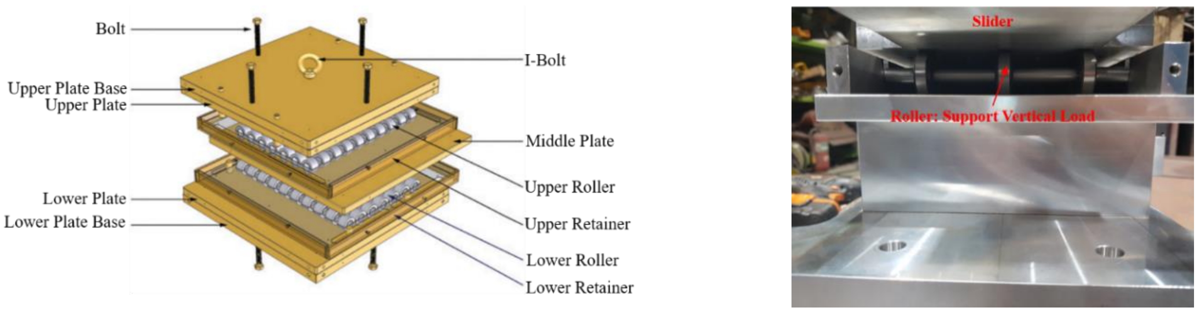

(a) (b)

Fig. 5 (a) Isolation roller bearing system (Park *et al*. 2013); (b) Roller/slider part of the proposed system

Table 2 Experimental conditions of dynamic characteristic tests

Experiment	Shear strain (%)	Frequency (Hz)	Cycle	Current (A)
Strain dependence	25, 50, 75, 100	0.5	10	0.0, 2.5, 5.0

Table 3 Information of the shaking table

	Values
Model	DY-HV-2000
Size	110 cm × 96 cm
Load	Max 600 kg
Max. acceleration	1.0 g
Max. velocity	21 cm/sec
Max. stroke	± 50 mm

3. Performance evaluation of the proposed hybrid base isolation system

3.1 Dynamic characteristic test of the proposed hybrid base isolation system

Dynamic characteristic tests of the proposed hybrid base isolation system were performed under the change of strain of the MRE and the change of the applied current. Dynamic characteristic tests were carried out in accordance with ISO 22762-1, taking into account the 100% strain of the shear modulus of the base isolation. The experimental conditions are tabulated in Table 2.

The excitation was applied to the sine wave with 0.5 Hz. The test system was composed of the shaking table, load cell (CAS SB-500L), amplifier (STT-200S-3), digital signal acquisition (NI PXI-4461), and laser displacement meter (AWLG 120s) as shown in Fig. 6. When the excitation (i.e., frequency, amplitude) is set in the shaking table according to the strain of the MRE, the force generated in the MRE-based base isolation system is transmitted to the load cell through the steel rod shown in Fig. 6. As a result, displacement–shear force hysteresis curves can be obtained according to the test conditions as shown in Fig. 8. The related information of the shaking table is tabulated in Table 3.

To exclude the Mullins effect, more than 50 times of excitations were performed to confirm the accuracy of test at the maximum strain (20 mm). The MR effect was calculated from the shear force-displacement hysteresis curve by referring to ISO 22762-1 as shown in Fig. 7.

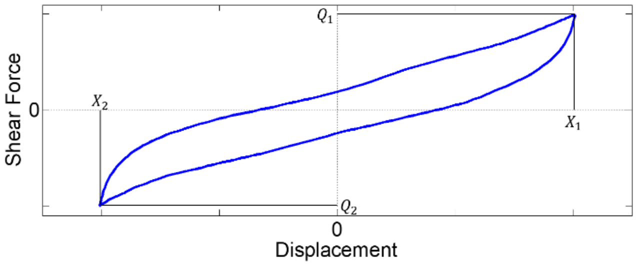

Fig. 7 Shear force-displacement hysteresis curve

From the hysteresis curve, the Eq. (1) can be translated into Eq. (2). The effective shear stiffness (K_{eff}) can be calculated as

$$K_{eff} = \frac{Q_1 - Q_2}{X_1 - X_2} \tag{2}$$

where Q_1 and Q_2 are the maximum/minimum shear force. X_1 and X_2 are the maximum / minimum displacement.

The shear force-displacement hysteresis curves from the experiment are shown in Fig. 8 and the related effective stiffness and MR effects are tabulated in Table 4. The maximum MR effect was 63.0% at 25% strain (5 mm), and 22.6% at 100% strain (20 mm), respectively.

Table 4 shows the calculated values of the effective shear stiffness for each condition and the MR effect at each strain. As can be seen from the Table 4, the effective shear stiffness decreases with increasing strain. This is due to the stress-strain relationship of the MRE, which has a linear relationship when the strain is relatively small, but the effective shear stiffness is gradually decreased because it decreases nonlinearly as the strain increases (Li *et al*. 2013). Also, it can be seen that the decrease of the effective shear stiffness becomes larger when the magnetic field is applied. This is because when the magnetic is applied to the MRE, the magnetic particles array inside the MRE forms chain structure. However, as the strain increases, the gap between the chain structure of the magnetic particles becomes wider resulting in the larger loss of the magnetic flux density in the MRE. Therefore, when the magnetic field is applied, the reduction of the MR effect decreases more significantly

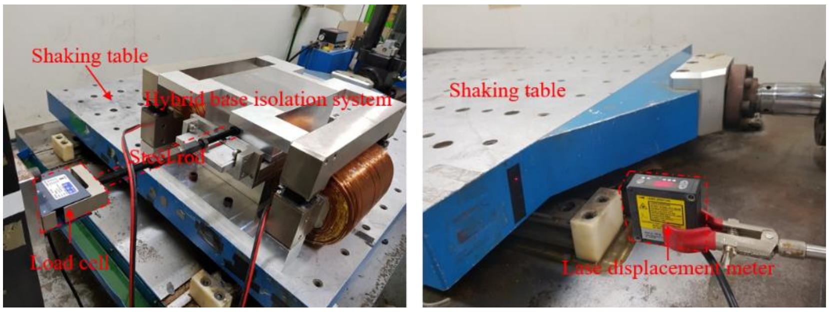

Fig. 6 Experimental set-up for dynamic characteristic test

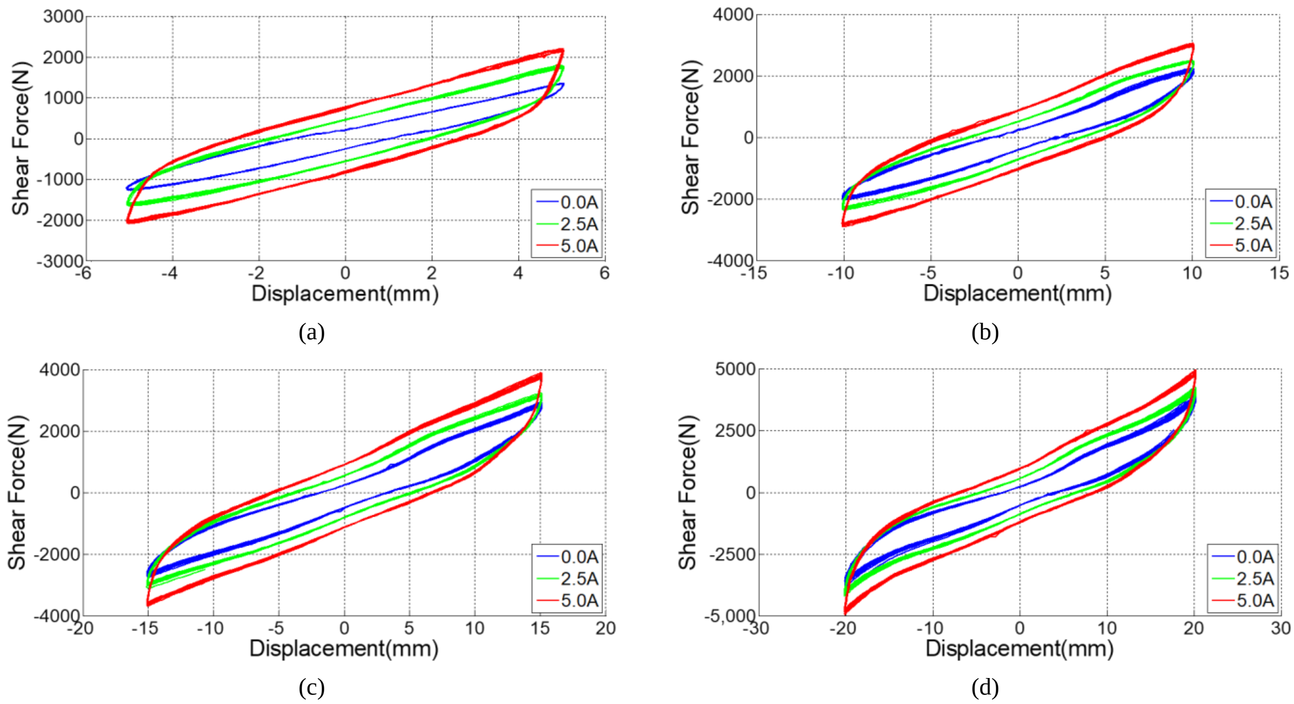

Fig. 8 Shear force-displacement hysteresis curves (strain: 25~100%, frequency: 0.5 Hz)

Table 4 The MR effect of the proposed hybrid base isolation system

		Strain (%)	25	50	75	100
Current (A)	0.0	Effective shear stiffness (kN/m)	262.97	213.21	207.27	201.33
	5.0	Effective shear stiffness (kN/m)	421.54	337.51	244.16	246.83
		MR effect (%)	60.3	58.3	17.8	22.6

in the large strain of the MRE.

To address this problem, it is important to minimize the loss of the magnetic flux density at large strain. In this study, the integrated MRE was used, resulting in the larger loss of the magnetic flux density compared with the laminated MRE with steel plate due to the low permeability of the MRE. Therefore, it is possible to minimize the reduction of the MR effect depending on the strain by constructing the laminated MRE with steel plate.

3.2 Hybrid simulation system

Although the proposed hybrid base isolation system is of a size to be tested on the shaking table, tens of tons of structures are suitable for the seismic design cycle (Son 2008). Therefore, it is difficult to fabricate and test the actual target structure, so performance evaluation was carried out through the hybrid simulation. The hybrid simulation is the combined method between experiment and numerical simulation. By combining experiment and numerical simulation, hybrid simulation can be used to validate full-scale structures of virtual structures that are difficult to verify experimentally (Nakashima 2001, Chen *et al.* 2019). The behavior of the base isolation system based on the MRE is nonlinear and uncertain in many cases, so it is important to consider the actual behavior rather than the numerical simulation. However, the numerical simulation can be implemented when the behavior is simple and the uncertainty is low for relatively large and heavy structure (Lee 2018). In this study, a two-story shear building is constructed as a numerical simulation. A simulation was performed by inputting the relative displacement of the foundation layer to the ground caused by the earthquake into the shaking table associated with the actual base isolation system. The control force of the hybrid base isolation system is input to the load cell and then applied to the foundation layer of the virtual structure to be practically circulated. Fig. 9 shows the block diagram of the hybrid simulation.

In Fig. 9, blue line indicates the hybrid simulation and green line is the part related to the semi-active control. Matlab Simulink Desktop Real-time program was used for the hybrid simulation. Data acquisition and signal output were performed using the NI PCIe-6321 DAQ card and NI SCB68A connector block, and the control force was measured via the CAS load cell SB-500L and STT-200S03 amplifiers as shown in Fig. 10.

3.3 Target structure

In order to evaluate the seismic performance of the proposed hybrid base isolation system, a three-degree-of

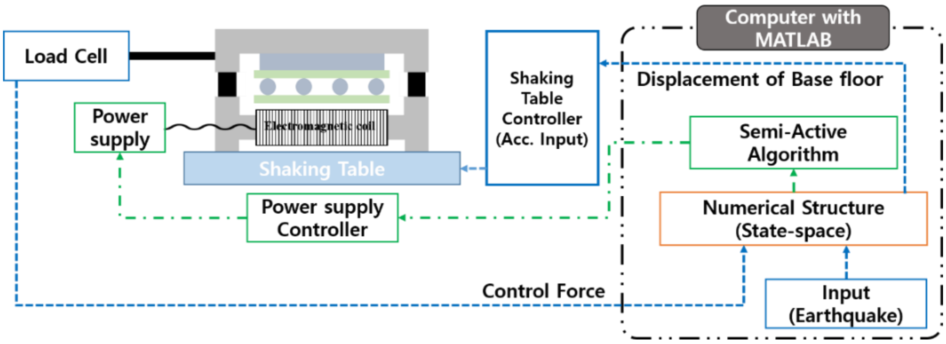

Fig. 9 Block diagram of hybrid simulation

Fig. 10 Physical part of experiment

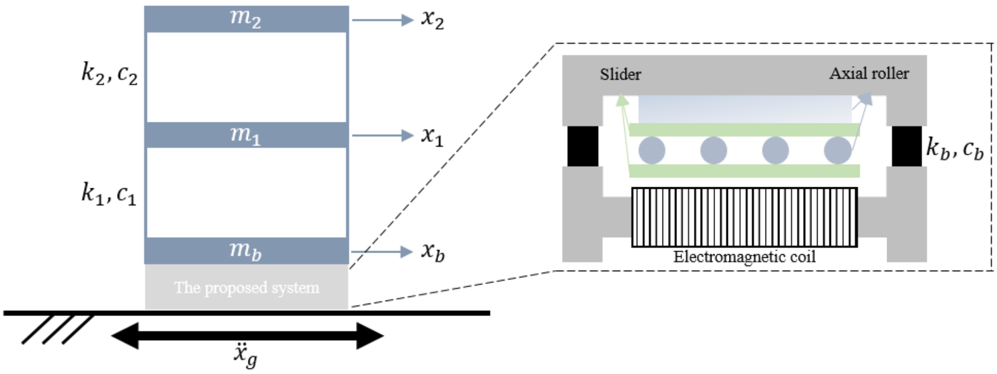

Fig. 11 Target structure (two-story-structure)

Table 5 Material properties of target structure

	Mass (kg)	Horizontal stiffness (kN/m)	Damping ratio	1st natural frequency (Hz)
Base	5,000	-		
1st floor	5,000	2,500	2%	2.2 (Without base isolation)
2nd floor	5,000	2,500		

freedom (3 DOF) structure was constructed by adding a foundation layer to a two-story building as shown in Fig. 11. The proposed hybrid base isolation system is designed to be installed in each column of target structure, but in this experiment, a hybrid simulation was performed by placing a two-story building on one hybrid base isolation system. The related material properties of the target structures are tabulated in Table 5.

The equation of motion for 3 DOF structure with a hybrid base isolation system can be expressed as

$$\boldsymbol{M}\ddot{\boldsymbol{x}} + \boldsymbol{C}\dot{\boldsymbol{x}} + \boldsymbol{K}\boldsymbol{x} = -\boldsymbol{M}\boldsymbol{\Gamma}\ddot{x}_g + \boldsymbol{\Lambda}f \quad (3)$$

where $\boldsymbol{x}$, $\dot{\boldsymbol{x}}$, and $\ddot{\boldsymbol{x}}$ are the relative displacement, velocity, and acceleration vector of structure to ground, respectively. $\boldsymbol{\Gamma}$ is unit vector, $\ddot{x}_g$ is earthquake acceleration. $\boldsymbol{\Lambda}$ is position vector, and f is a control force of the base isolation. $\boldsymbol{M}$, $\boldsymbol{C}$, and $\boldsymbol{K}$ are mass, damping, and stiffness matrix, respectively.

$$\boldsymbol{M} = \begin{bmatrix} m_b & 0 & 0 \\ 0 & m_1 & 0 \\ 0 & 0 & m_2 \end{bmatrix},$$
$$\boldsymbol{C} = \begin{bmatrix} c_b + c_1 & -c_1 & 0 \\ -c_1 & c_1 + c_2 & -c_2 \\ 0 & -c_2 & c_2 \end{bmatrix}, \quad (4)$$

$$\boldsymbol{K} = \begin{bmatrix} k_b + k_1 & -k_1 & 0 \\ -k_1 & k_1 + k_2 & -k_2 \\ 0 & -k_2 & k_2 \end{bmatrix} \tag{4}$$

From the above equation of motion, the state vector is defined as

$$\boldsymbol{z} = \begin{bmatrix} \boldsymbol{x} \\ \dot{\boldsymbol{x}} \end{bmatrix} \tag{5}$$

To obtain the relative displacement, velocity, and acceleration vector of structure to ground, the output vector is defined as

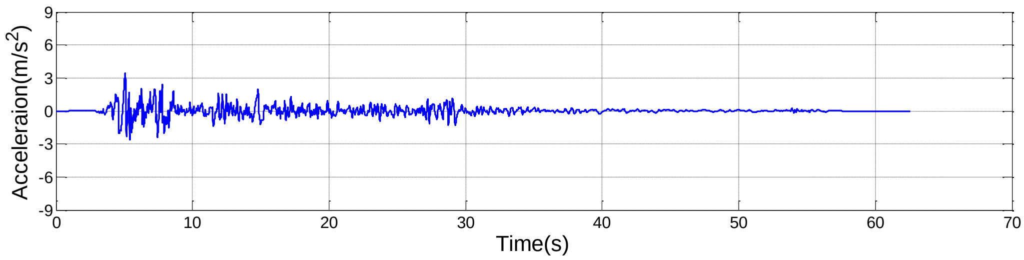

(a) El Centro earthquake (1940)

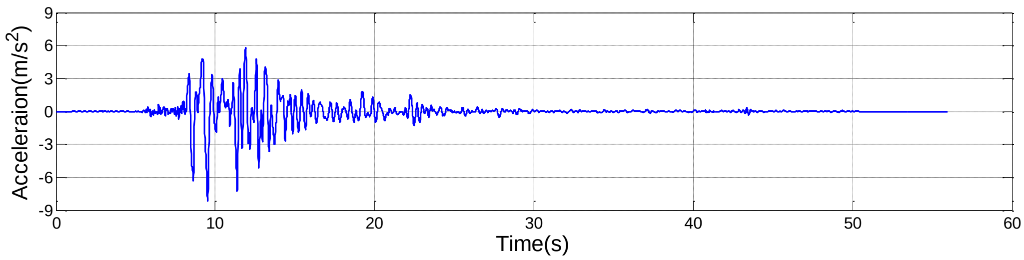

(b) Kobe earthquake (1995)

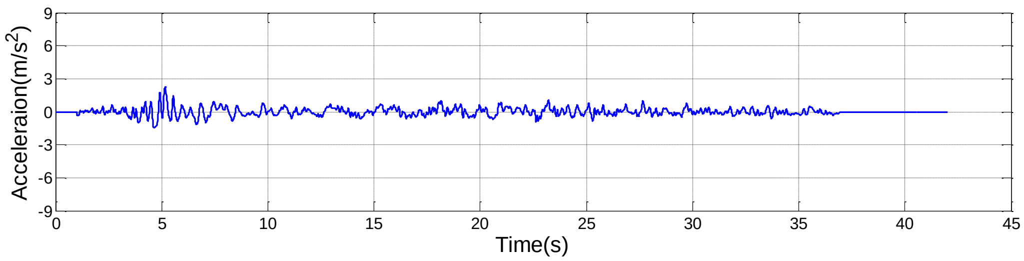

(c) Hachinohe earthquake (1968)

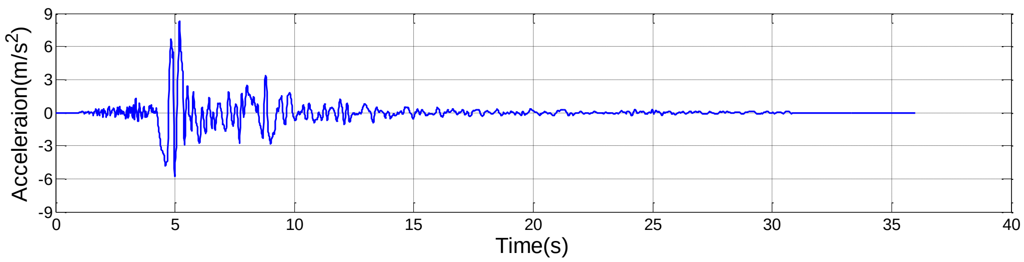

(d) Northridge earthquake (1994)

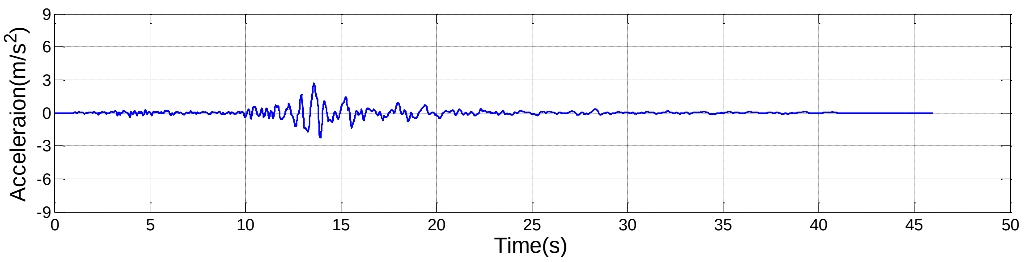

(e) Loma Prieta earthquake (1989)

Fig. 12 Historical earthquakes ground acceleration

$$\dot{\boldsymbol{z}} = \boldsymbol{A}\boldsymbol{z} + \boldsymbol{B}f + \boldsymbol{E}\ddot{x}_g,\ \ \boldsymbol{y} = \boldsymbol{C}'\boldsymbol{z} + \boldsymbol{D}f + \boldsymbol{F}\ddot{x}_g \tag{6}$$

where, matrices $\boldsymbol{A}, \boldsymbol{B}, \boldsymbol{C}', \boldsymbol{D}, \boldsymbol{E},$ and $\boldsymbol{F}$ are as follows

$$\boldsymbol{A} = \begin{bmatrix} \boldsymbol{0}_{3\times3} & \boldsymbol{I}_{3\times3} \\ -\boldsymbol{M}^{-1}\boldsymbol{K} & -\boldsymbol{M}^{-1}\boldsymbol{C} \end{bmatrix}, \quad \boldsymbol{B} = \begin{bmatrix} \boldsymbol{0}_{3\times3} \\ \boldsymbol{M}^{-1}\boldsymbol{\Lambda} \end{bmatrix},$$

$$\boldsymbol{C}' = \begin{bmatrix} \boldsymbol{I}_{3\times3} & \boldsymbol{0}_{3\times3} \\ \begin{bmatrix} 1 & 0 & 0 \\ -1 & 1 & 0 \\ 0 & -1 & 1 \end{bmatrix} & \boldsymbol{0}_{3\times3} \\ \boldsymbol{0}_{3\times3} & \boldsymbol{I}_{3\times3} \\ -\boldsymbol{M}^{-1}\boldsymbol{K} & -\boldsymbol{M}^{-1}\boldsymbol{C} \end{bmatrix}, \tag{7}$$

$$\boldsymbol{D} = \begin{bmatrix} \boldsymbol{0}_{3\times1} \\ \boldsymbol{0}_{3\times1} \\ \boldsymbol{0}_{3\times1} \\ \boldsymbol{M}^{-1}\boldsymbol{\Lambda} \end{bmatrix}, \quad \boldsymbol{F} = \begin{bmatrix} \boldsymbol{0}_{3\times1} \\ \boldsymbol{0}_{3\times1} \\ \boldsymbol{0}_{3\times1} \\ \boldsymbol{0}_{3\times1} \end{bmatrix}$$

3.4 Input earthquakes

To evaluate the performance of the proposed hybrid base isolation system, the hybrid simulation was carried out under five earthquakes (i.e., El Centro earthquake (1940), Kobe earthquake (1995), Hachinohe earthquake (1968), Northridge earthquake (1994), and Loma Prieta earthquake (1989)). The time-acceleration history is shown in Fig. 12.

3.5 Control type

The performance of the proposed hybrid base isolation system was evaluated for various earthquakes as mentioned above chpater. The performance evaluation was carried out through 'Power-off', 'Power-on', and semi-active 'Fuzzy' control; (a) 'Power-off' indicates the base isolation system that works without the applied current, (b) 'Power-on' indicates the base isolation system that works with the applied current (5 A), (c) 'Fuzzy' indicates the base isolation system that works with an isolator controlled by fuzzy control algorithm. The semi-active fuzzy control algorithm uses IF-THEN rules in Simulink to operate the power supply to apply the current in each electromagnetic closed circuit. The semi-active fuzzy control algorithm is designed to determine the current applied to the electromagnetic closed circuits according to the relative displacement between base and 2nd floor, the base floor displacement, and the scaled earthquake velocity data (Yang *et al*. 2016). Each displacement and velocity are expressed in two forms; P-Positive, and N-Negative. The output current signal is also defined as; L-Large, and S-Small. Table 6 shows the rules based on the inputs. Detailed fuzzy control algorithm is referred in Yang *et al*. (2016).

Table 6 The rules of the fuzzy logic (Yang *et al*. 2016)

Variable	Indicated form							
$x_2 - x_b$	N	N	N	N	P	P	P	P
x_b	N	P	N	P	N	P	N	P
$\dot{x}_g$	P	P	N	N	P	P	N	N
Current	S	L	S	L	L	S	L	S

3.6 Experiment and result

This section presents the performance evaluation results of the proposed hybrid base isolation system using the hybrid simulation. Before comparing the results according to the control type, the results were compared according to the presence and absence of the base isolation system by free vibration. The hybrid simulation was performed in the case of the presence of the base isolation system, and the system without the base isolation system was performed numerical simulation to obtain the acceleration responses as shown in Fig. 13. In the case of the absence of the base isolation system, it can be seen that the acceleration response is extensively large compared to the base isolation system. Therefore, the performance evaluation was carried out based on the results of the control type.

In the previous section, three types of control method were described; (a) 'Power-off', (b) 'Power-on', and (c) semi-active 'Fuzzy' control. For each earthquake input, the responses of the structure were obtained to compare the results of each control type method. Fig. 14 shows the acceleration responses of the top floor (2nd floor) for each earthquake. Also, Table 7 indicates the absolute maximum acceleration response at 2nd floor and the relative ratio compared with passive type "Power-off".

In El Centro earthquake, the acceleration responses of the structure controlled by 'Fuzzy' control are reduced overall period of earthquake expect for the 10~15 sec. In the case of Kobe and Northridge earthquakes such as pulse form, the reduction of the acceleration responses of the structure of each control type is similar to the input earthquake. In particular, in both earthquakes, the acceleration responses of the structure through the 'Fuzzy' appear to be located between 'Power-on' and 'Power-off'. The reason is that the constructed semi-active fuzzy control algorithm is based on the relative displacement difference

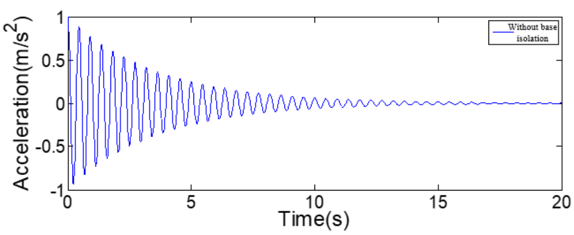

(c)

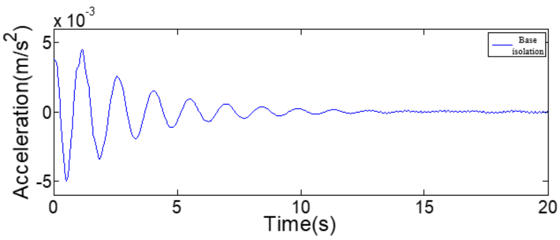

(d)

Fig. 13 Acceleration response of 2nd floor; (a) without base isolation system; (b) base isolation system

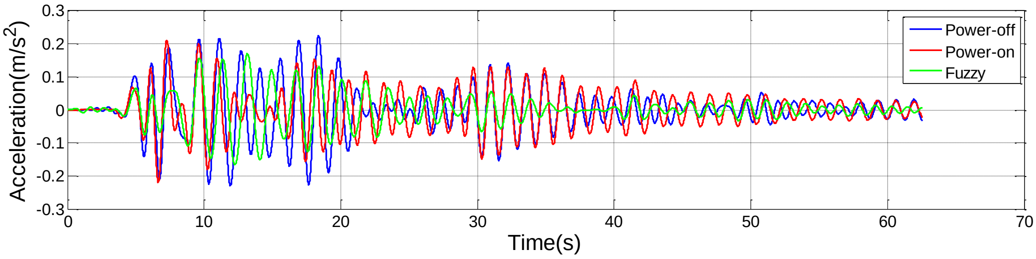

(a) El Centro earthquake (1940)

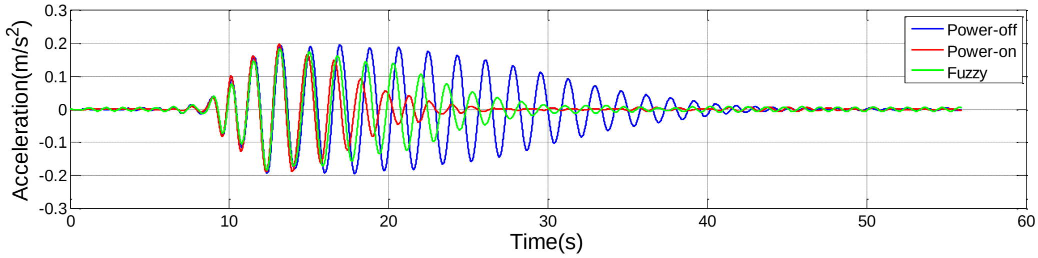

(b) Kobe earthquake (1995)

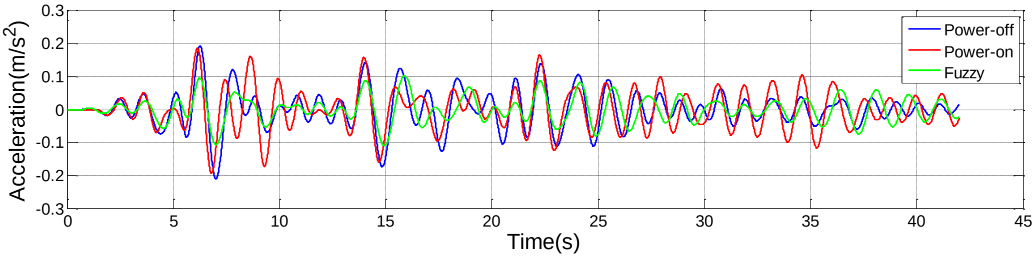

(c) Hachinohe earthquake (1968)

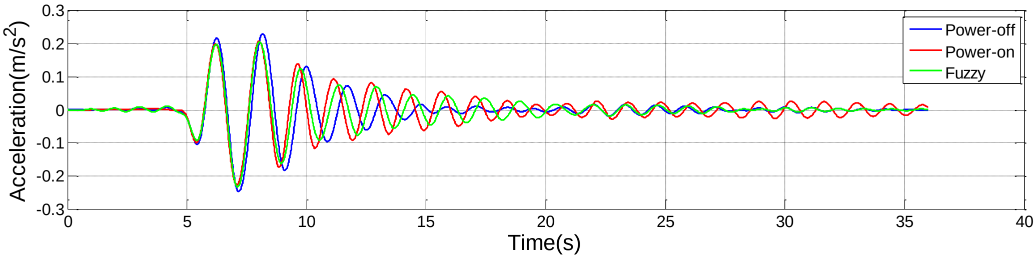

(d) Northridge earthquake (1994)

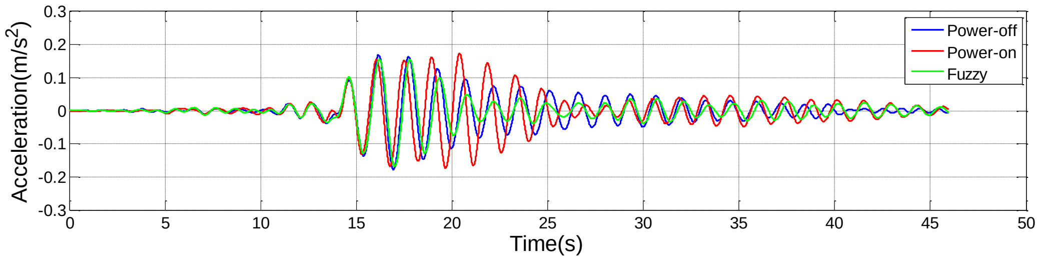

(e) Loma Prieta earthquake (1989)

Fig. 14 The absolute acceleration responses of 2nd floor under input earthquakes

between base and 2nd floor, the base floor displacement, and the scaled earthquake velocity data. In the case of Hachinohe earthquake, 'Fuzzy' control greatly reduces the acceleration response of the structure during the entire period. This is can be confirmed that not only the acceleration responses but also the relative displacement and the displacement of the base isolation system are significantly reduced. In Loma Prieta earthquake, it is confirmed that the acceleration response of the structure through 'Fuzzy' is the smallest and remarkably reduced during the entire period even though the acceleration responses of the structure are similar to that of Kobe and

Table 7 Maximum acceleration of 2nd floor

Earthquake	Power-off (m/s^2)	Power-on (m/s^2)	Fuzzy (m/s^2)
El Centro	0.2307 (-)	0.2210 (-4.20%)	0.1703 (-26.12%)
Kobe	0.1957 (-)	0.1976 (0.97%)	0.1840 (-5.98%)
Hachinohe	0.2108 (-)	0.1944 (-7.78%)	0.1096 (-48.01%)
Northridge	0.2477 (-)	0.2271 (-8.32%)	0.2341 (-5.4%)
Loma Prieta	0.1779 (-)	0.1734 (-2.53%)	0.1694 (-4.78%)

Northridge earthquakes. However, unlike the two earthquakes, it can be seen that the acceleration response reduction through 'Fuzzy' decreases after 20 sec. This confirms that the constructed fuzzy control algorithm is limited to pulse type seismic acceleration. Nevertheless, 'Fuzzy' for each seismic acceleration reduced the acceleration of the structure compared to the passive type.

Fig. 15 shows the relative displacement when occurring the maximum relative displacement between base and 2nd floor. The maximum relative displacement between the base and 2nd floor has a minimum value in 'Fuzzy'. Also, when comparing with the passive type, 'Power-off' shows a relatively smaller relative displacement response between base and 2nd floor than 'Power-on'. In the case of 'Fuzzy' and 'Power-off', the relative displacement response decreased due to the rubber material properties acting as the base isolation system. However, in the case of 'Power-on', since the MRE became relatively stiff, the relative displacement increased because the MRE did not function as the base isolation system. In contrast to the acceleration response, 'Power-off' is significantly reduced compared to 'Power-on'. Also, it can be seen that the displacement response of the structure through fuzzy is reduced remarkably compared with passive types. The reason is that the semi-active fuzzy control algorithm is constructed using the displacement difference between the base and 2nd floor, so that the reduction in relative displacement is larger than passive types.

The maximum deformation of the MRE and the ratio compared with 'Power-off' are tabulated in Table 8. The maximum deformation of the MRE was largest value in the 'Power-off', which is a conventional passive type rubber bearing system. Also, the control was performed outside of the maximum strain range of the MRE in Northridge earthquake. For performance evaluation, several responses

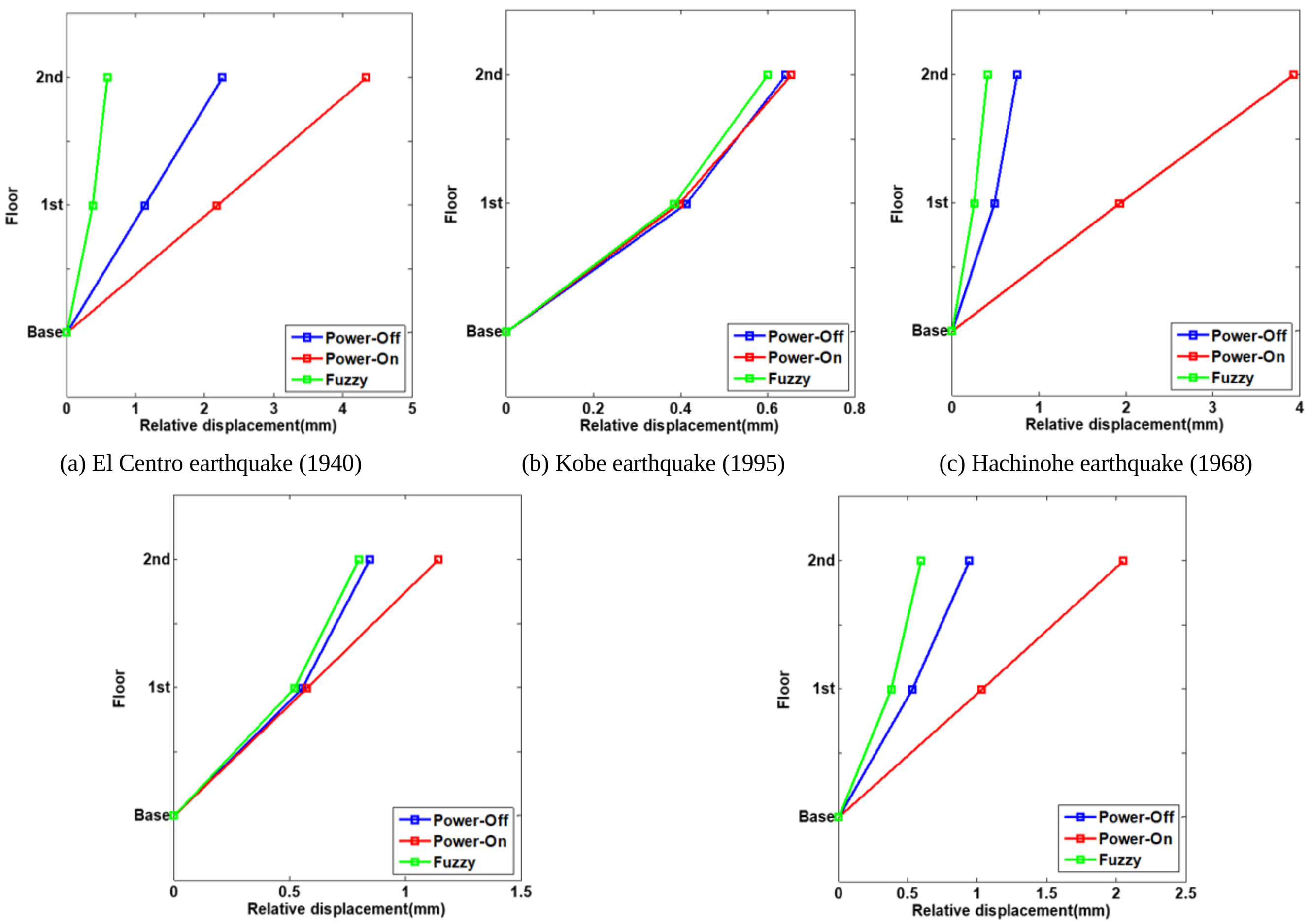

(a) El Centro earthquake (1940)
(b) Kobe earthquake (1995)
(c) Hachinohe earthquake (1968)
(d) Northridge earthquake (1994)
(e) Loma Prieta earthquake (1989)

Fig. 15 The maximum relative displacement between base and 2nd floor

Table 8 Maximum deformation of the MRE

Earthquake	Power-off (m/s^2)	Power-on (m/s^2)	Fuzzy (m/s^2)
El Centro	13.3102 (-)	11.2429 (-15.5%)	13.2748 (0.27%)
Kobe	16.7403 (-)	14.7456 (-11.9%)	14.7238 (-12.05%)
Hachinohe	12.2949 (-)	10.4744 (-14.81%)	7.0274 (-42.84%)
Northridge	23.3793 (-)	18.9687 (-18.87%)	19.1506 (-18.09%)
Loma Prieta	12.3931 (-)	9.6321 (-22.28%)	12.1488 (-1.97%)

of the structure were obtained to compare the passive and semi-active fuzzy control using the hybrid simulation. The comparison was performed based on the results of the acceleration of the 2nd floor, the relative displacement between base and 2nd floor and the deformation of the MRE. For Kobe and Northridge earthquakes such as pulse type earthquake, there is a limitation of the semi-active fuzzy control algorithm used in this paper, but the responses of the structure are reduced compared to the passive type for all earthquakes.

4. Conclusions

In this paper, a new hybrid base isolation system consisting of the MRE and roller bearing which has adaptability to various earthquakes and considers practical applicability has been proposed. The proposed hybrid base isolation system is composed of the MRE electromagnetic closed circuits and roller bearing. The roller part was constructed to support the vertical load so that the vertical load was not applied to the MRE. In other words, the MRE can perform a significant contribution to the control of horizontal direction. The MRE electromagnetic circuits are designed to be installed in the free space of the roller bearing and can form a strong magnetic field in the MRE. The roller/slider part is designed to be able to move in two axes and is designed taking into account the maximum strain of the MRE.

Dynamic characteristic tests have been performed under the change of strain of the MRE and the change of the applied current. It was carried out considering the 100% strain of the MRE according to ISO 22762-1. From the tests, as the strain increases, the MR effect decreases. This is because the reduction of the effective shear stiffness (K_{eff}) is larger when the magnetic field is applied. The MRE has low permeability, and the effective shear stiffness decreases sharply due to the larger loss of the magnetic flux density in the MRE as the strain increases. The laminated MRE with steel plate is one of factors that can address this problem. Performance evaluation under representative earthquakes (i.e., El Centro, Kobe, Hachinohe, Northridge, and Loma Prieta earthquake) have been carried out through the three types of control method (i.e., “Power-off”, “Power-on”, and “Fuzzy”) using the hybrid simulation. The acceleration of the 2nd floor, the relative displacement between the base and 2nd floor, and the deformation of the MRE responses were compared for each control type for the performance evaluation. From the results, it was confirmed that the responses of the structure were effectively reduced in the semi-active ‘Fuzzy’ control algorithm. From the dynamic characteristic tests and performance evaluation of the proposed hybrid base isolation system, the feasibility and possibility for the hybrid base isolation applications have been demonstrated despite some considerations for performance improvements.

Acknowledgments

This work was supported by the National Research Foundation Korea (NRF) grant funded by the Korea government (MSIP) (NRF-2019R1A2C2007835 and No. 2017R1A5A1014883).

References

Behrooz, M., Wang, X.J. and Gordaninejad, F. (2014a), “Modeling of a new semi-active/passive magnetorheological elastomer isolator”, *Smart Mater. Struct.*, **23**(4), 045013. https://doi.org/10.1088/0964-1726/23/4/045013

Behrooz, M., Wang, X.J. and Gordaninejad, F. (2014b), “Performance of a new magnetorheological elastomer isolation system”, *Smart Mater. Struct.*, **23**(4), 045014. https://doi.org/10.1088/0964-1726/23/4/045014

Chen, L., Gong, X.L., Jiang, W.Q., Yao, J.J., Deng, H.X. and Li, W.H. (2007), “Investigation on magnetorheological elastomers based on natural rubber”, *J. Mater. Sci.*, **42**(14), 5483-5489. https://doi.org/10.1007/s10853-006-0975-x

Chen, P.C., Hsu, S.C., Zhong, Y.J. and Wang, S.J. (2019), “Real-time hybrid simulation of smart base-isolated raised floor systems for high-tech industry”, *Smart Struct. Syst., Int. J.*, **23**(1), 91-106. https://doi.org/10.12989/sss.2019.23.1.091

Clutch, M.F. and Rabinow, J. (1948), “Technical News Bulletin”, *National Bureau of Standards*, **32**(4), 7.

Davis, L.C. (1999), “Model of magnetorheological elastomers”, *J. Appl. Phys.*, **85**(6), 3348-3351. https://doi.org/10.1063/1.369682

Domizio, M.N., Ambrosini, D. and Curadelli, O. (2019), “TMD effectiveness in nonlinear RC structures subjected to near fault earthquakes”, *Smart Struct. Syst., Int. J.*, **24**(4), 447-457. https://doi.org/10.12989/sss.2019.24.4.447

Ginder, J.M., Nichols, M.E., Elie, L.D. and Clark, S.M. (2000), “Controllable-stiffness components based on magnetorheological elastomers”, *Proceedings of SPIE’s 7th Annual International Symposium onsmart Structurs and Materials*: *Smart Structures and Integrated Systems*, Newport Beach, CA, USA, March, **3985**, 418-425. https://doi.org/10.1117/12.388844

Jangid, R.S. and Kelly, J.M. (2001), “Base isolation for near-fault motions”, *Earthq. Eng. Struct. Dyn.*, **30**(5), 691-707. https://doi.org/10.1002/eqe.31

Jolly, M.R., Carlson, J.D. and Munoz, B.C. (1996), “A model of the behaviour of magnetorheological materials”, *Smart Mater. Struct.*, **5**(5), 607-614. https://doi.org/10.1088/0964-1726/5/5/009

Jung, H.J., Eem, S.H., Jang, D.D. and Koo, J.H. (2011), “Seismic performance analysis of a smart base-isolation system considering dynamics of MR elastomers”, *J. Intel. Mater. Syst. Struct.*, **22**(13), 1439-1450.

https://doi.org/10.1177/1045389X11414224
Lee, C.W. (2018), “Development of Smart Base Isolation System Based on MR Elastomer and Evaluation of Its Seismic Performance”, Master’s Thesis; Korea Advanced Institute of Science and Technology (KAIST), Korea.
Lee, C.W., Kim, I.H. and Jung, H.J. (2018), “Fabrication and characterization of natural rubber-based magnetorheological elastomers at large strain for base isolators”, *Shock Vib*., 7434536. https://doi.org/10.1155/2018/7434536
Li, Y. and Li, J. (2019), “Overview of the development of smart base isolation system featuring magnetorheological elastomer”, *Smart Struct. Syst., Int. J.*, **24**(1), 37-52. https://doi.org/10.12989/sss.2019.24.1.037
Li, Y., Li, J., Li, W. and Samali, B. (2013), “Development and characterization of a magnetorheological elastomer based adaptive seismic isolator”, *Smart Mater. Struct*., **22**(3), 035005. https://doi.org/10.1088/0964-1726/22/3/035005
Li, Y., Li, J., Li, W. and Du, H. (2014), “A state-of-the-art review on magnetorheological elastomer devices”, *Smart Mater. Struct*., **23**(12), 123001. https://doi.org/10.1088/0964-1726/23/12/123001
Liao, G.J., Gong, X.L., Kang, C.J. and Xuan, S.H. (2011), “The design of an active-adaptive tuned vibration absorber based on magnetorheological elastomer and its vibration attenuation performance”, *Smart Mater. Struct*., **20**(7), 075015. https://doi.org/10.1088/0964-1726/20/7/075015
Lokander, M. and Stenberg, B. (2003), “Performance of isotropic magnetorheological rubber materials”, *Polym. Test*., **22**(3), 245-251. https://doi.org/10.1016/S0142-9418(02)00043-0
Naeim, F. and Kelly, J.M. (1999), *Design of Seismic Isolated Structures*: *from Theory to Practice*, John Wiley & Sons.
Nagarajaiah, S. (2006), “Structural control benchmark problem: Smart base isolated building subjected to near fault earthquakes”, *Structural Control and Health Monitoring: The Official Journal of the International Association for Structural Control and Monitoring and of the European Association for the Control of Structures*, **13**(2-3), 571-572. https://doi.org/10.1002/stc.98
Nakashima, M. (2001), “Development, potential, and limitations of real-time online (pseudo-dynamic) testing”, *Philosophical Transactions of the Royal Society of London. Series A: Mathematical, Physical and Engineering Sciences*, **359**(1786), 1851-1867. https://doi.org/10.1098/rsta.2001.0876
Opie, S. and Yim, W. (2011), “Design and control of a real-time variable modulus vibration isolator”, *J. Intel. Mater. Syst. Struct*., **22**(2), 113-125. https://doi.org/10.1177/1045389X10389204
Park, Y.G., Ha, S.H., Seong, M.S., Jeon, J. and Choi, S.B. (2013), “Roller design of IRB Seismic Isolation Device Using Testing Evaluation: Part I. Geometry Dimension and Crowning”, *Transaction of the Korean Society for Noise and Vibration Engineering*, **23**(2), 185-191. https://doi.org/10.5050/KSNVE.2013.23.2.185
Rabinow, J. (1951), “Magnetic fluid torque and force transmitting device”, U.S. Patent No. 2,575,360.
Ramallo, J.C., Johnson, E.A. and Spencer, B.F. (2002), "“Smart” base isolation systems”, *J. Eng. Mech*., **128**(10), 1088-1099. https://doi.org/10.1061/(ASCE)0733-9399(2002)128:10(1088)
Ruddy, C., Ahearne, E. and Byme, G. (2012), “A review of magnetorheological elastomers: properties and applications”, *Advanced Manufacturing Science (AMS) Research*, 20.
Skineer, R.I., Robinson, W.H. and McVerry, G.H. (1993), *An Introduction to Seismic Isolation*, John Wiley & Sons.
Son, I.C. (2008), “IRB System Used for Rollers to Protect Building from Earthquake”, *Computat. Struct. Eng*., **21**(4), 61-66.
Tiong, P.L., Kelly, J.M. and Or, T.T. (2017), “Design approach of high damping rubber bearing for seismic isolation”, *Smart Struct. Syst*., *Int. J*., **20**(3), 303-309. https://doi.org/10.12989/sss.2017.20.3.303
Wongprasert, N. and Symans, M.D. (2005), “Experimental evaluation of adaptive elastomeric base-isolated structures using variable-orifice fluid dampers”, *J. Struct. Eng*., **131**(6), 867-877. https://doi.org/10.1061/(ASCE)0733-9445(2005)131:6(867)
Yang, J., Sun, S.S., Tian, T.F., Li, W.H., Du, H.P., Alici, G. and Nakano, M. (2016), “Development of a novel multi-layer MRE isolator for suppression of building vibrations under seismic events”, *Mech. Syst. Signal Process*., **70**, 811-820. https://doi.org/10.1016/j.ymssp.2015.08.022
Yoshioka, H., Ramallo, J.C. and Spencer, B.F. (2002), "“Smart” base isolation strategies employing magnetorheological dampers”, *J. Eng. Mech*., **128**(5), 540-551. https://doi.org/10.1061/(ASCE)0733-9399(2002)128:5(540)
Zhang, X.Z. and Li, W.H. (2009), “Adaptive tuned dynamic vibration absorbers working with MR elastomers”, *Smart Struct. Syst.*, *Int. J*., **5**(5), 517-529. https://doi.org/10.12989/sss.2009.5.5.517
Zhu, W. and Rui, X.T. (2014), “Semiactive vibration control using a magnetorheological damper and a magnetorheological elastomer based on the Bouc-Wen model”, *Shock Vib*., 405421. https://doi.org/10.1155/2014/405421.

BS